Electronic Supplementary Material (ESI) for New Journal of Chemistry.

Manganese(II) bromo- and iodo-complexes with phosphoramidate and phosphonate ligands: synthesis, characterization and photoluminescence

Marco Bortoluzzi, Jesús Castro, Andrea Di Vera, Alberto Palù and Valentina Ferraro

Electronic Supplementary Information

Table S1 Crystal data and structure refinement for **$[MnX_2(OP^{NOO})_2]$** (X = Br, I).

Compound	$[MnBr_2(OP^{NOO})_2]$	$[MnI_2(OP^{NOO})_2]$
Empirical formula	$C_{28}H_{32}Br_2MnN_2O6P_2$	$C_{28}H_{32}I_2MnN_2O_6P_2$
Formula weight	769.25	863.23
Temperature	100(2) K	100(2) K
Wavelength	0.71073 Å	0.71073 Å
Crystal system	Monoclinic	Monoclinic
Space group	$P2_1/c$	$P2_1/n$
Unit cell dimensions	a = 17.2910(15) Å	a = 10.0153(8) Å
	b = 10.3838(9) Å	b = 17.3133(14) Å
	c = 18.4599(15) Å	c = 19.6665(16) Å
	β = 103.825(3)°	β = 103.495(3)°
Volume	3218.4(5) $Å^3$	3316.0(5) $Å^3$
Z	4	4
Density (calculated)	1.588 Mg/m^3	1.729 Mg/m^3
Absorption coefficient	3.035 mm^{-1}	2.398 mm^{-1}
F(000)	1548	1692
Crystal size	0.233 x 0.212 x 0.023 mm	0.191 x 0.091 x 0.069 mm
Theta range for data collection	2.267 to 28.320°	2.353 to 28.383°
Index ranges	$-23 \le h \le 23$	$-13 \le h \le 13$
	$-13 \le k \le 13$	$-23 \le k \le 23$
	$-24 \le l \le 24$	$-11 \le l \le 26$
Reflections collected	84590	8310
Independent reflections	7976 [R_{int} = 0.0637]	8310 [R_{int} = 0.0426]
Reflections observed (>2σ)	6849	7024
Data Completeness	0.997	0.992
Absorption correction	Semi-empirical from equivalents	Semi-empirical from equivalents
Max. and min. transmission	0.7457 and 0.5152	0.7457 and 0.6383
Refinement method	Full-matrix least-squares on F^2	Full-matrix least-squares on F^2
Data / restraints / parameters	7976 / 0 / 374	8310 / 0 / 375
Goodness-of-fit on F^2	1.030	1.119
Final R indices [$I>2\sigma(I)$]	R_1 = 0.0284	R_1 = 0.0472
	wR_2 = 0.0627	wR_2 = 0.1777
R indices (all data)	R_1 = 0.0377	R_1 = 0.0589
	wR_2 = 0.0660	wR_2 = 0.1889
Largest diff. peak and hole	0.475 and -0.483 e.$Å^{-3}$	1.321 and -1.744 e.$Å^{-3}$

Manganese(II) bromo- and iodo-complexes with phosphoramidate and phosphonate ligands: synthesis, characterization and photoluminescence

Marco Bortoluzzi, Jesús Castro, Andrea Di Vera, Alberto Palù and Valentina Ferraro

Table S2 Crystal data and structure refinement for **$[Mn_2Br_4(\mu\text{-}OP^{NNO\sim ONN}PO)_2]$** and **$[MnI_2(\mu\text{-}OP^{NNO\sim ONN}PO)]_n$**.

Compound	$[Mn_2Br_4(\mu\text{-}OP^{NNO\sim ONN}PO)_2]$	$[MnI_2(\mu\text{-}OP^{NNO\sim ONN}PO)]_n$
Empirical formula	C14 H28 Br2 Mn N4 O4 P2	C14 H28 I2 Mn N4 O2 P2
Formula weight	593.10	655.08
Temperature	100(2) K	100(2) K
Wavelength	0.71073 Å	0.71073 Å
Crystal system	Monoclinic	Monoclinic
Space group	$P2_1/c$	$P2_1/n$
Unit cell dimensions	a = 11.7628(14) Å	a = 11.1151(9) Å
	b = 9.0147(10) Å	b = 14.0317(12) Å
	c = 23.078(3) Å	c = 16.0386(14) Å
	β = 103.072(4)°	β = 100.395(3)°
Volume	2383.7(5) Å^3	2460.4(4) Å^3
Z	4	4
Density (calculated)	1.653 Mg/m^3	1.768 Mg/m^3
Absorption coefficient	4.065 mm^{-1}	3.190 mm^{-1}
F(000)	1188	1268
Crystal size	0.133 x 0.115 x 0.071 mm	0.265 x 0.238 x 0.205 mm
Theta range for data collection	2.811 to 28.506°	2.362 to 28.345°
Index ranges	$-15 \le h \le 15$	$-14 \le h \le 14$
	$-12 \le k \le 12$	$-18 \le k \le 18$
	$-21 \le l \le 30$	$-20 \le l \le 21$
Reflections collected	5934	50220
Independent reflections	5934 [R_{int} = 0.0736]	6143 [R_{int} = 0.0425]
Reflections observed (>2σ)	5147	5510
Data Completeness	0.989	0.999
Absorption correction	Semi-empirical from equivalents	Semi-empirical from equivalents
Max. and min. transmission	0.7151 and 0.5810	0.7457 and 0.5007
Refinement method	Full-matrix least-squares on F^2	Full-matrix least-squares on F^2
Data / restraints / parameters	5934 / 0 / 255	6143 / 0 / 252
Goodness-of-fit on F^2	1.162	1.093
Final R indices [$I>2\sigma(I)$]	R_1 = 0.0906	R_1 = 0.0395
	wR_2 = 0.2264	wR_2 = 0.0960
R indices (all data)	R_1 = 0.1004	R_1 = 0.0458
	wR_2 = 0.2304	wR_2 = 0.0986
Largest diff. peak and hole	1.512 and -1.732 e.Å^{-3}	1.946 and -2.470 e.Å^{-3}

Table S3 Selected bond lengths [Å] and angles [°] for **[$MnX_2(OP^{NOO})_2$]** complexes.

	X=Br	X=I
Mn-X(1)	2.4479(4)	2.6788(9)
Mn-X(2)	2.4760(4)	2.6786(9)
Mn-O(11)	2.0416(14)	2.029(4)
Mn-O(21)	2.0525(14)	2.035(4)
P(1)-N(1)	1.6104(18)	1.623(5)
P(1)-O(11)	1.4755(14)	1.477(4)
P(1)-O(12)	1.5773(14)	1.580(4)
P(1)-O(13)	1.5692(14)	1.567(4)
P(2)-O(21)	1.4767(14)	1.474(4)
P(2)-O(22)	1.5721(14)	1.576(4)
P(2)-O(23)	1.5818(14)	1.572(4)
P(2)-N(2)	1.6102(17)	1.620(5)
X(1)-Mn-X(2)	117.168(14)	112.28(3)
O(11)-Mn-O(21)	97.90(6)	93.39(19)
O(11)-Mn-X(1)	112.74(4)	111.40(12)
O(11)-Mn-X(2)	108.86(4)	113.53(12)
O(21)-Mn-X(1)	105.40(4)	113.58(12)
O(21)-Mn-X(2)	113.12(4)	111.38(13)
P(1)-O(11)-Mn	176.14(10)	175.2(3)
P(2)-O(21)-Mn	164.73(10)	174.7(3)

Table S4 Selected bond lengths [Å] and angles [°] for **[$Mn_2Br_4(\mu\text{-}OP^{NNO\sim ONN}PO)_2$]** and **[$MnI_2(\mu\text{-}OP^{NNO\sim ONN}PO)]_n$**.

	[$Mn_2Br_4(\mu\text{-}OP^{NNO\sim ONN}PO)_2$]	**[$MnI_2(\mu\text{-}OP^{NNO\sim ONN}PO)]_n$**
Mn-X(1)	2.4653(17)	2.6742(7)
Mn-X(2)	2.4597(18)	2.6489(7)
Mn-O(11)	2.047(7)	2.035(3)
Mn-O(22^{i})	2.053(7)	2.036(3)
P(1)-N(11)	1.614(9)	1.618(4)
P(1)-N(12)	1.643(9)	1.626(4)
P(1)-O(11)	1.479(8)	1.490(3)
P(1)-O(12)	1.596(7)	1.587(3)
P(2)-N(21)	1.601(11)	1.620(4)
P(2)-N(22)	1.605(9)	1.620(4)
P(2)-O(21)	1.590(7)	1.585(3)
P(2)-O(22)	1.486(7)	1.495(3)
X(1)-Mn-X(2)	119.66(7)	114.27(2)
O(11)-Mn-O(22^{i})	101.2(3)	99.42(13)
O(11)-Mn-X(1)	110.9(2)	110.52(9)
O(11)-Mn-X(2)	105.3(2)	107.30(9)
O(22^{i})-Mn-Br(1)	105.4(2)	111.71(9)
O(22^{i})-Mn-Br(2)	113.0(2)	112.50(9)
P(1)-O(11)-Mn	148.3(5)	143.4(2)
P(2)-O(22)-Mn^{ii}	138.5(5)	145.7(2)

Symm. Op.: For **[$Mn_2Br_4(\mu\text{-}OP^{NNO\sim ONN}PO)_2$]**: i=ii, 2-x, 1-y, 1-z; for **[$MnI_2(\mu\text{-}OP^{NNO\sim ONN}PO)]_n$**, O(22i) should be read as O(12i): i, 0.5-x, y-0.5, 1.5-z; ii, 0.5-x, y+0.5, 1.5-z.

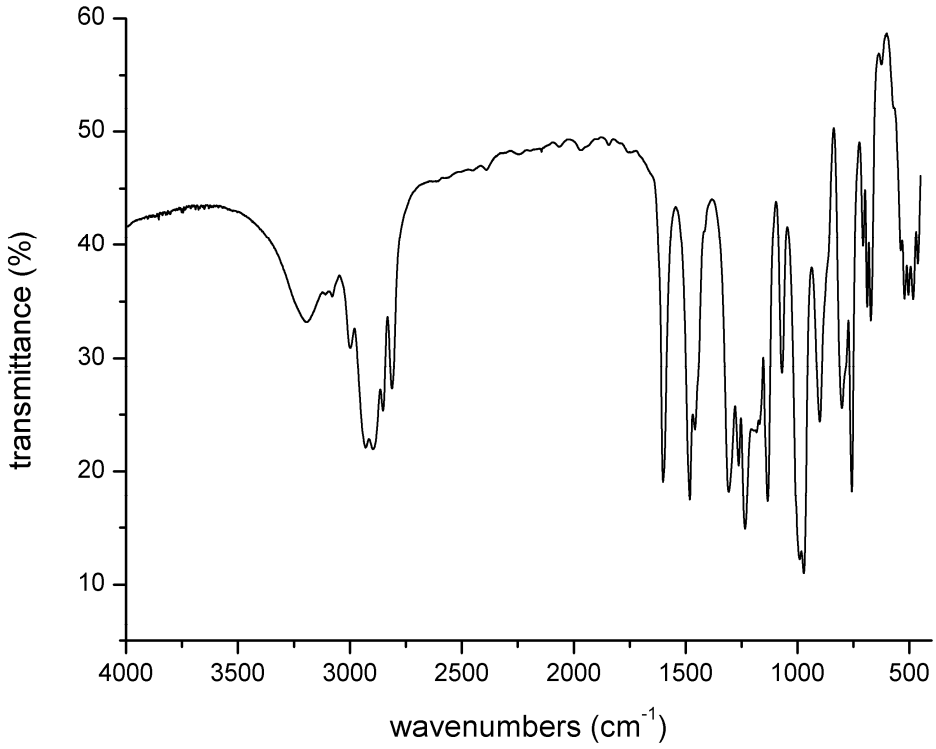

Fig. S1 IR spectrum of **OP$^{NNO\frown ONN}$PO**.

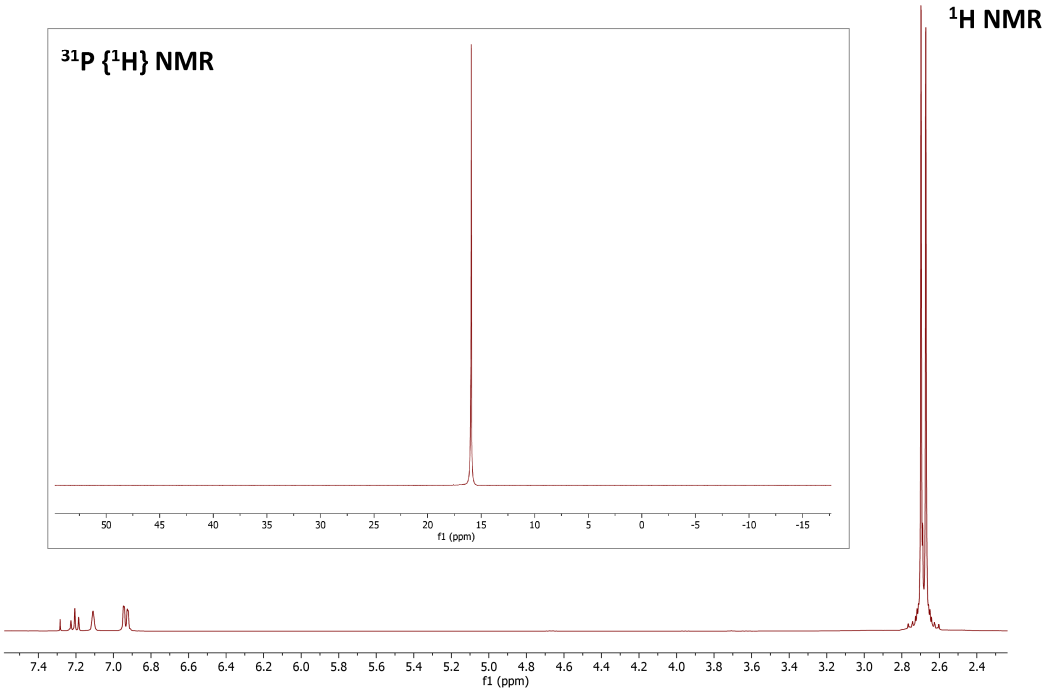

Fig. S2 ^{1}H NMR and ^{31}P $\{^{1}$H$\}$ NMR spectra of **OP$^{NNO\frown ONN}$PO**.

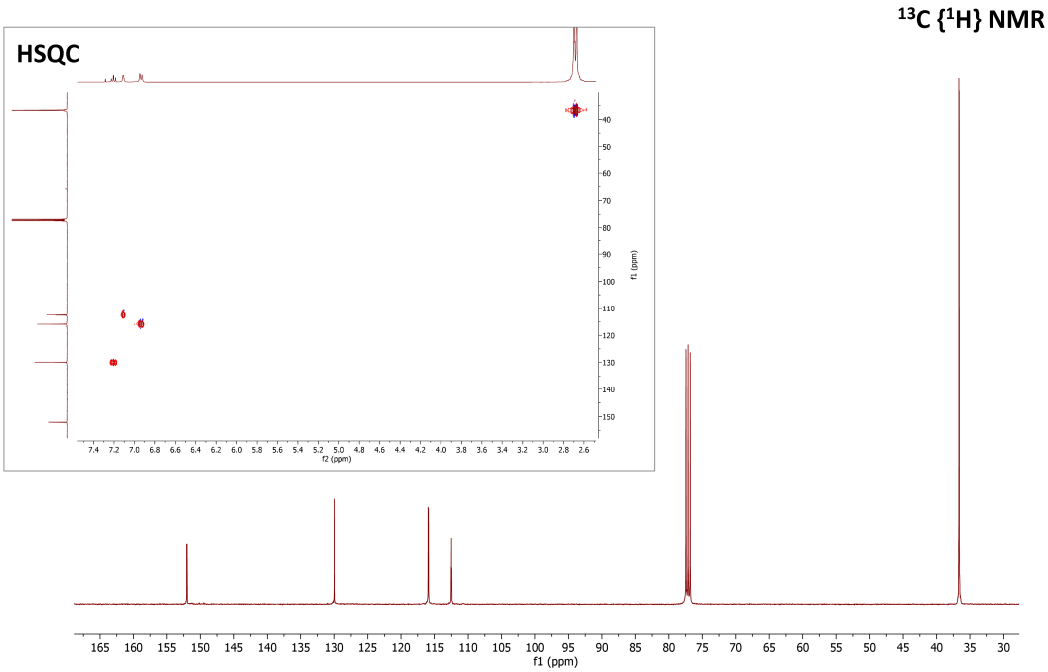

Fig. S3 ^{13}C {^{1}H} NMR and HSQC-edited spectra of **OP$^{NNO\sim ONN}$PO** ($CDCl_3$, 300 K).

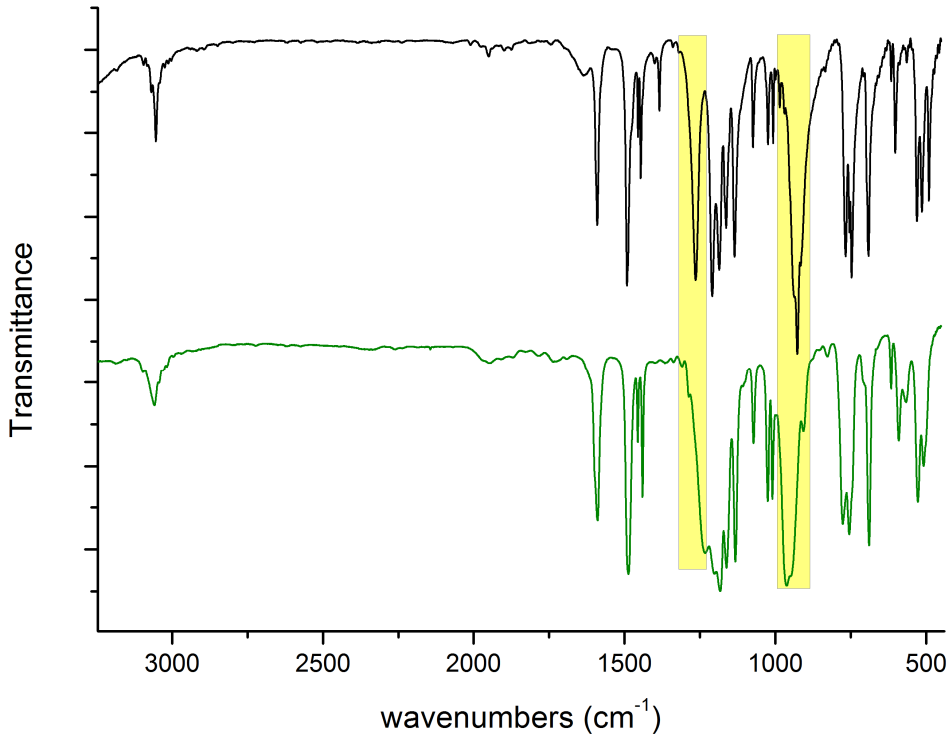

Fig. S4 IR spectra of **OP^{COO}** (black line) and **[$MnBr_2${OP^{COO}}$_2$]** (green line) with $\nu_{P=O}$ and ν_{P-O} regions highlighted.

Description of monomeric of $[MnX_2(OP^{NOO})_2]$ complexes and their supramolecular network

The Mn(II) complexes contain two **OP^{NOO}** ligands coordinated through the phosphoryl oxygen atom and two halide atoms. The coordination polyhedron is best described in both the compounds as a slightly distorted tetrahedron, as expected for this kind of complexes and indicated in the main text. Evidences are the τ_4 parameter[2] values of 0.91, [X=Br] and 0.94, [X=I] (the extreme values are 0.00 for a square planar geometry and 1.00 for a perfect tetrahedron), and the dihedral angle between the perpendicular planes MnX_2 and MnO_2, 85.71(4)° [X=Br] and 88.34(9)°[X=I].

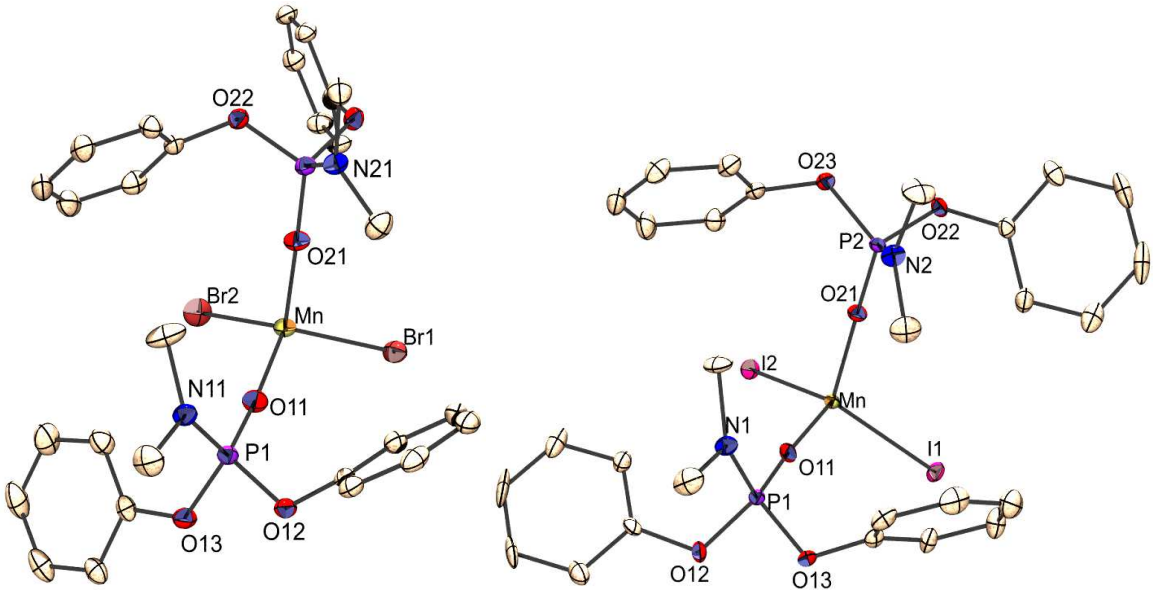

Fig. S5 ORTEP[1] plots of the **$[MnX_2(OP^{NOO})_2]$** the compounds.

As can be seen in Figure S5 (and in the main text), the disposition of one of the ligands differs because of a twist around a P–O bond. Figure S6 shows a superimposition of these compounds to display the differences, that revealed to be important in the supramolecular network of the compounds, as it will be described below.

The NMe_2 groups are expected to be pyramidal, but in these complexes they are almost planar, the nitrogen atom is only 0.088(2) and 0.127(2) Å [X = Br] or 0.112(5) and 0.150(7) Å [X = I] out of the plane formed by the two carbon atoms and the phosphorus one. These values are quite different with respect to those measured for pyramidal NMe_2 groups in related complexes.[3]

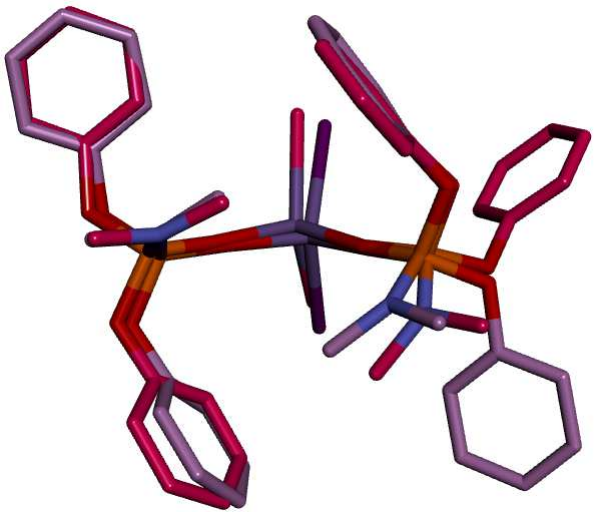

Fig. S6 Superimposition of the **[$MnX_2(OP^{NOO})_2$]** complexes, showing on the right the different orientation of the phenyl rings.

The disposition of the ligands previously mentioned allows, only in **[$MnI_2(OP^{NOO})_2$]**, interactions between the oxygen atom O(13) and the C(41) to C(46) ring [symm. op. x-1, y, z; distance between the centroid and the oxygen atom of 3.427(4) Å, distance from O(13) to the plane 3.20 Å] and between O(23) and the C(21) to C(26) ring [symm. op. 1+x, y, z; distance Ct-O(23), 3.344(4) Å; distance from O(23) to the plane 3.15 Å]. The interactions are sketched in Figure S7.

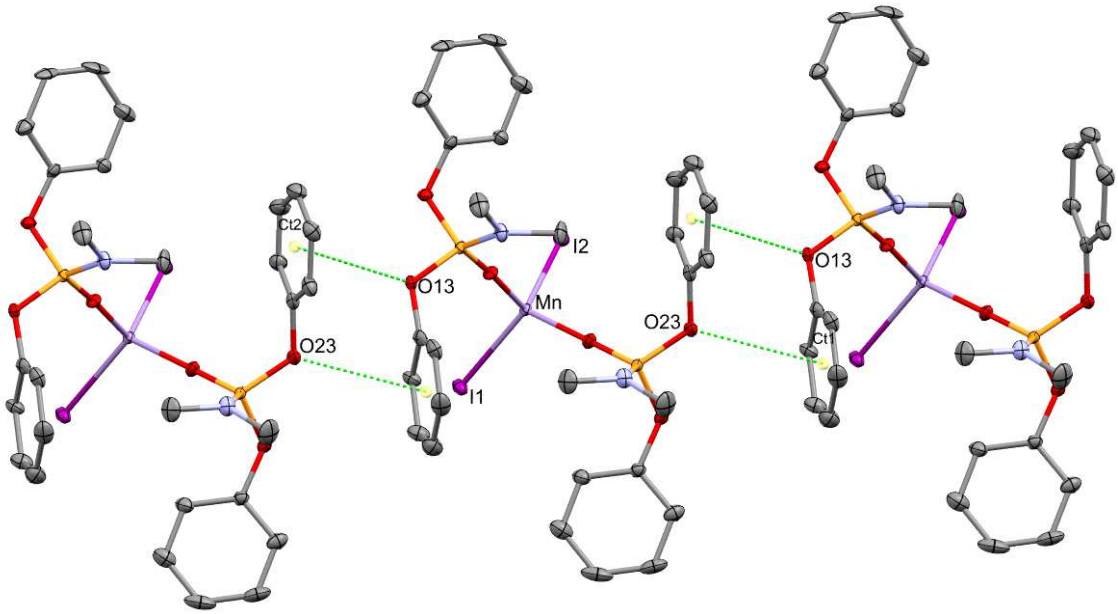

Fig. S7 Packing of **[$MnI_2(OP^{NOO})_2$]** complex.

In **[$MnI_2(OP^{NOO})_2$]** non-classical hydrogen bonds are also observable between iodine atoms and the methyl groups (see Figure S8). The related parameters are given in Table S5.

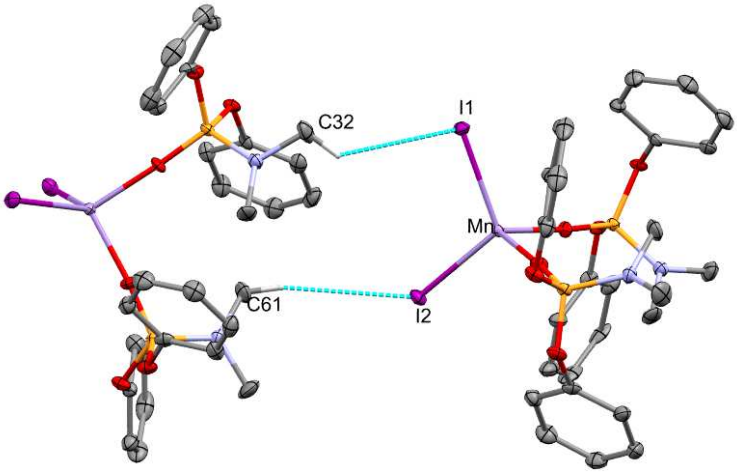

Fig. S8 Hydrogen bonds in **[$MnI_2(OP^{NOO})_2$]** complex.

Noteworthy, the above-mentioned O···rings interactions are not present in the bromide analogue. Instead, several non-classical hydrogen bonds can be found between a methyl of phenyl CH and a bromine atom (Figures S9-S10). The related parameters are given in Table S5.

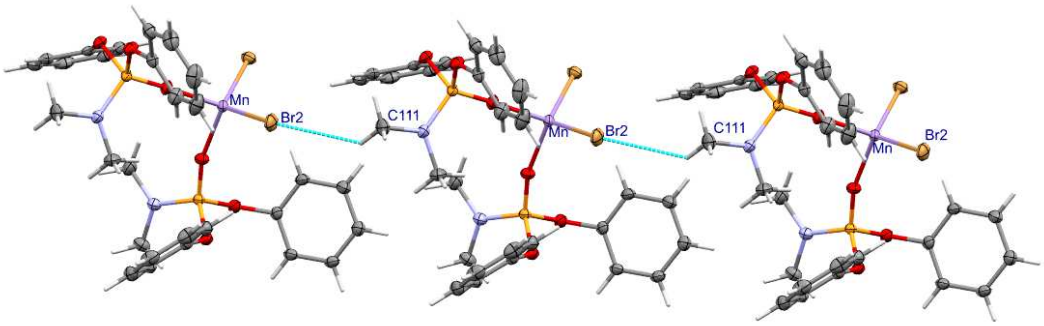

Fig. S9 Hydrogen bonds in **[$MnBr_2(OP^{NOO})_2$]** complex.

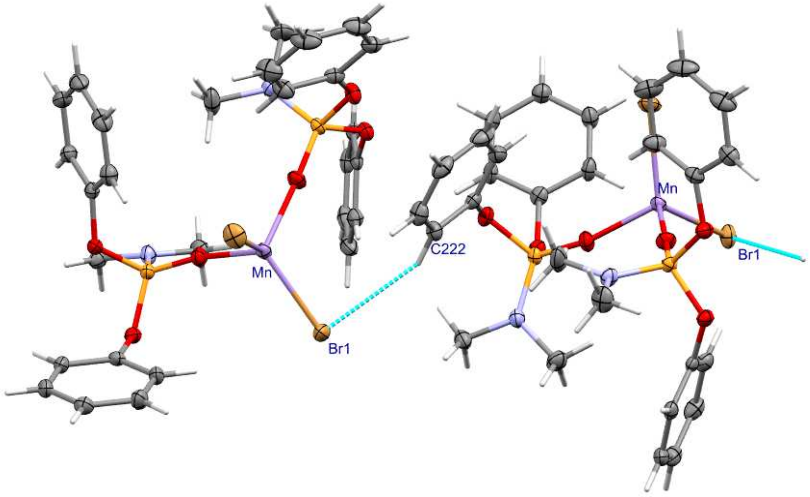

Fig. S10 Hydrogen bonds in **[$MnBr_2(OP^{NOO})_2$]** complex.

The supramolecular network is also maintained by the C-H···π interaction depicted in Figure S11. This relates the *ortho* carbon of one phenol group and the π cloud of a neighboring molecule [Symm. op. x, 3/2-y, 1/2+z]. The centroid of the ring is situated at 2.6 Å from the hydrogen atom, 3.451(2) Å from the carbon atom, forming a C-H···Ct angle of 149°.

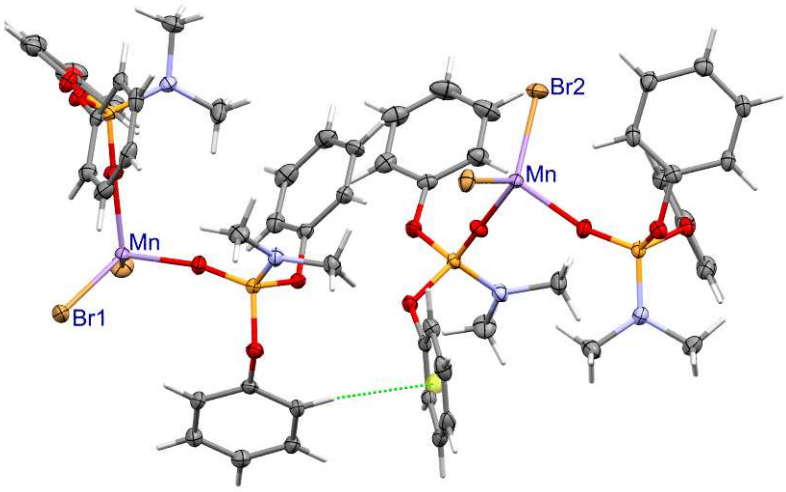

Fig. S11 C-H···π interaction in **[$MnBr_2(OP^{NOO})_2$]** complex.

Table S5 Hydrogen bonds for **[$MnX_2(OP^{NOO})_2$]** complexes [Å and°].

D-H...A	d(D-H)	d(H...A)	d(D...A)	<(DHA)
[$MnBr_2(OP^{NOO})_2$]				
C(111)-H(11A)...Br(2^{i})	0.98	2.99	3.544(2)	117.3
C(222)-H(222)...Br(1^{ii})	0.95	2.91	3.720(2)	144.1
[$MnI_2(OP^{NOO})_2$]				
C(32)-H(32A)...I(1^{iii})	0.98	3.24	3.951(7)	131.2
C(61)-H(61C)...I(2^{iii})	0.98	3.43	4.258(7)	143.6

Symmetry operations: i: x, y+1, z; ii, x, 3/2-y, z+1/2; iii, x-1/2, 3/2-y, z-1/2.

Description of $[Mn_2Br_4(\mu\text{-}OP^{NNO\sim ONN}PO)_2]$ and $[MnI_2(\mu\text{-}OP^{NNO\sim ONN}PO)]_n$ complexes and their supramolecular network

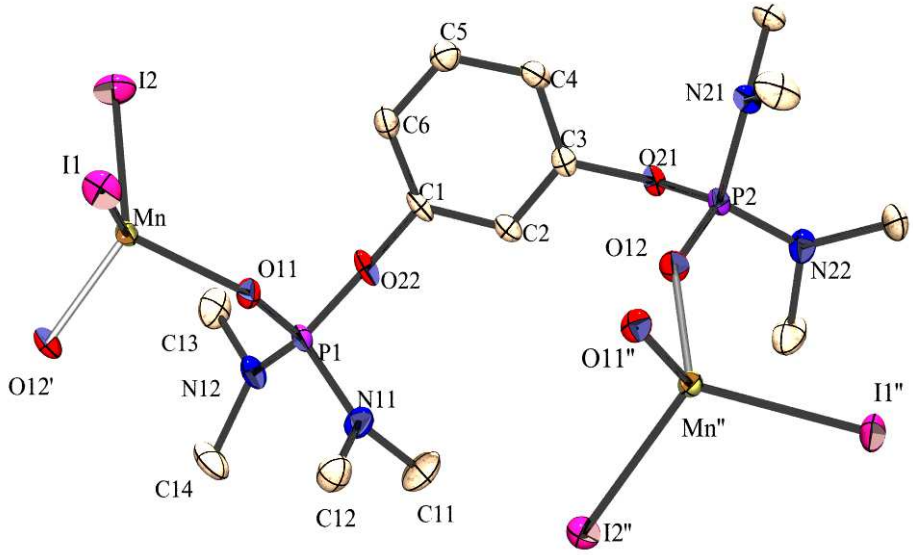

Fig. S12 The asymmetric unit and the closest atoms that continue the chain of $[MnI_2(\mu\text{-}OP^{NNO\sim ONN}PO)]_n$. Symmetry transformations used to generate equivalent atoms: i, 0.5-x, y-0.5, 1.5-z; ii, 0.5-x, y+0.5, 1.5-z.

In Figure S12[1] the asymmetric unit of $[MnI_2(\mu\text{-}OP^{NNO\sim ONN}PO)]_n$ is depicted as an example, together with the symmetry generated atom O(12^{i}), to show the Mn surrounding, the symmetry generated Mn^{ii} and the coordinated atoms. The symmetry operations that generate these atoms are given in the footnote of Figure S12. Figure S13 shows a superimposition of $[Mn_2Br_4(\mu\text{-}OP^{NNO\sim ONN}PO)_2]$ and $[MnI_2(\mu\text{-}OP^{NNO\sim ONN}PO)]_n$ [X=Br, carbon atoms in reddish; X=I, carbon atoms in purple], and demonstrates that a twist in a Mn-O bond generates small differences in the disposition of the halogen atoms (represented as spheres) allowing the diverse supramolecular arrangement. Indeed, as explained in the main text, only a dimeric structure was obtained for the bromide derivative, as shown in Figure S14.

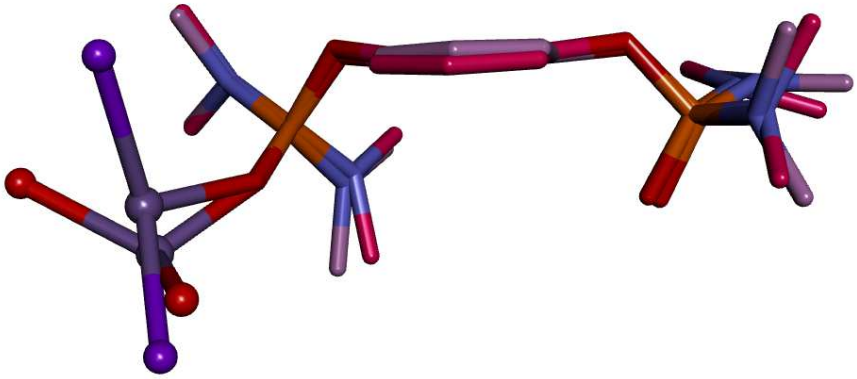

Fig. S13 Superimposition of **[Mn_2Br_4(μ-$OP^{NNO\sim ONN}PO)_2$]** and **[MnI_2(μ-$OP^{NNO\sim ONN}PO$)]$_n$**.

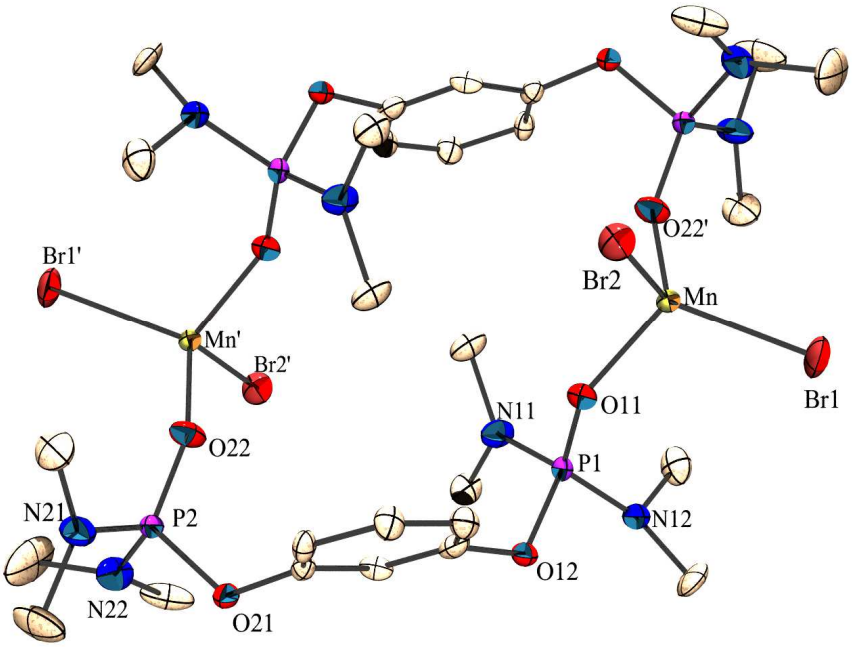

Fig. S14 ORTEP plot of **[Mn_2Br_4(μ-$OP^{NNO\sim ONN}PO)_2$]** complex.

On the other hand, Figure S15 shows part of the chain of the **[MnI_2(μ-$OP^{NNO\sim ONN}PO$)]$_n$** coordination polymer, characterized by a zigzag structure growing in the *y* axis. The distance between the nearest Mn atoms is 8.8446(9) Å, related to atoms in the same chain, longer than that found in the **[Mn_2Br_4(μ-$OP^{NNO\sim ONN}PO)_2$]** dimer, equal to 8.043(4) Å.

Dihedral angles between the MnX_2 and MnO_2 planes of 85.2(3)° [X=Br] and 88.46(7)°[X=I] (close to theoretical 90°), together with the τ_4 parameter[2] of 0.92 [X=Br] and 0.91 [X=I], confirm that the coordination polyhedron is best described as a slightly distorted tetrahedron.

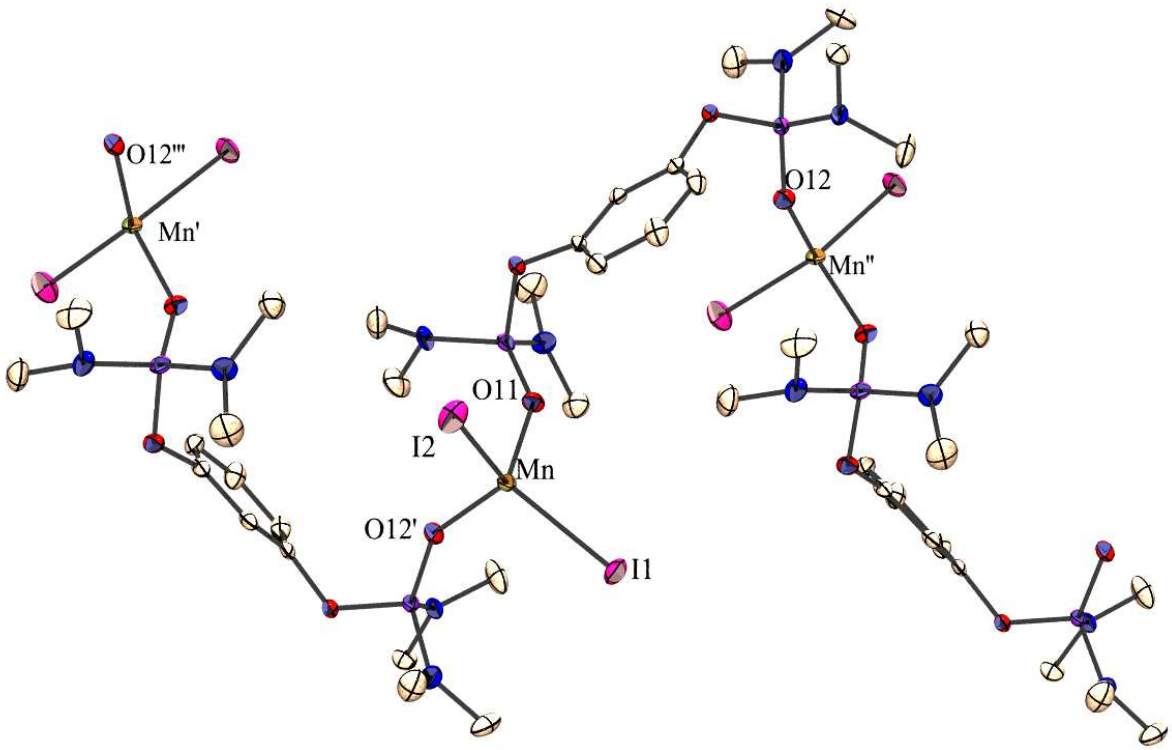

Fig. S15 Three asymmetric units to show the zigzag chain growing in the *y* axis.

We have previously found in the hexamethylphosphoramide (HMPA) compound $[MnBr_2\{O=P(NMe_2)_2\}_2]$[3] that, when three amides are bonded to a phosphorus atom, two of them are planar, but the third one shows some pyramidal shape. In the compounds described in this paper an oxygen atom replaces one of the amide groups, but similar situations can be found. In **$[Mn_2Br_4(\mu\text{-}OP^{NNO\sim ONN}PO)_2]$** the atom labeled as N(11) is 0.003(1) Å out of the C_2P plane (in other words, the atoms are almost coplanar), but the atom labeled as N(12) is 0.304(1) Å out of the plane. The values are 0.108(1) Å and 0.217 Å for the corresponding N(21) and N(22), respectively. In the case of **$[MnI_2(\mu\text{-}OP^{NNO\sim ONN}PO)]_n$** one of the amide group bonded to P(1) is almost planar [N(11) deviates only 0.13(1) Å of the plane formed by the carbon and the phosphorus atom], while the other is clearly pyramidal [N(12) deviated up to 0.35(1) Å of such plane]. Atom P(2) is bonded to N(21) and N(22), and both the nitrogen atoms are clearly pyramidal, deviating 0.73(1) and 0.51(1) Å, respectively. The P(1)-O(22)-C(1) and P(2)-O(21)-C(3) angles are however virtually the same and the angles between the plane of the benzene and the C-O bonds do not show significant differences [O(22)-C(1), 6.5(3)° and O(21)-C(3), 4.7(3)°].

The supramolecular network for **[Mn_2Br_4(μ-$OP^{NNO\sim ONN}PO)_2$]** is maintained by some non-classical hydrogen bond, detailed in Table S6 and represented in Figures S16 and S17.

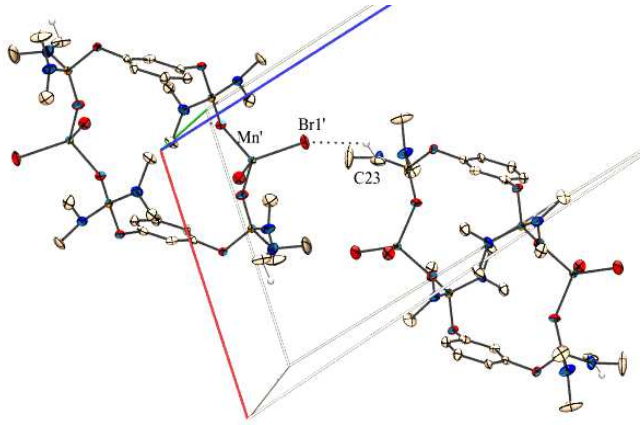

Fig. S16 C-H···Br bond found in **[Mn_2Br_4(μ-$OP^{NNO\sim ONN}PO)_2$]** complex.

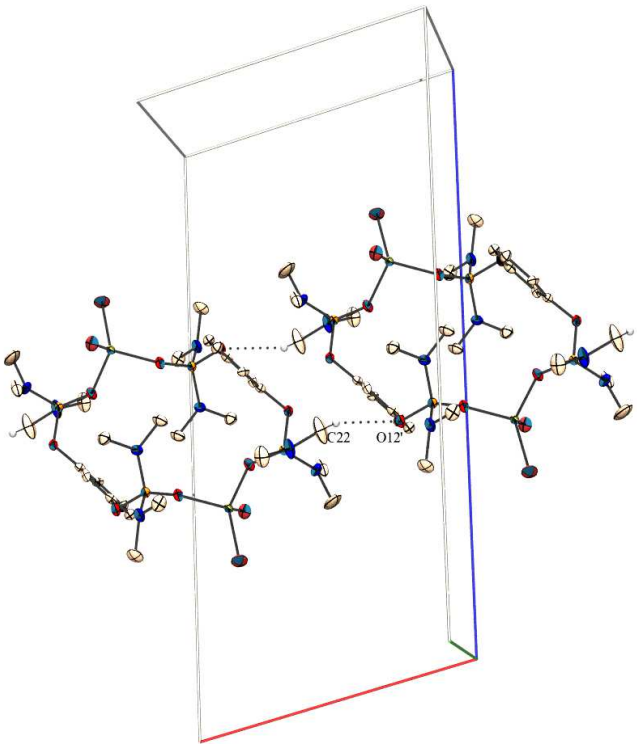

Fig. S17 C-H···O bond found in **[Mn_2Br_4(μ-$OP^{NNO\sim ONN}PO)_2$]** complex.

In the polymeric **[MnI_2(μ-$OP^{NNO\sim ONN}PO$)]$_n$** compound two parallel chains are connected by weak hydrogen bonds between the methyl groups and the electronegative oxygen atoms or the sterically not hindered iodine atoms. The parameters of these interactions, shown in Figure S18, are given in Table S6.

Table S6 Hydrogen bonds for polymeric complexes [Å and °].

D-H...A	d(D-H)	d(H...A)	d(D...A)	<(DHA)
$[Mn_2Br_4(\mu\text{-}OP^{NNO\sim ONN}PO)_2]$				
C(23)-H(23C)...Br(2^{i})#1	0.98	3.07	3.859(14)	138.2
C(22)-H(22B)...O(12^{ii})#2	0.98	2.78	3.667(19)	151.2
$[MnI_2(\mu\text{-}OP^{NNO\sim ONN}PO)]_n$				
C(21)-H(21B)...O(22^{i})	0.98	2.65	3.400(5)	133.4
C(24)-H(24A)...I(1^{ii})	0.98	3.40	4.058(5)	126.6
C(12)-H(12C)...I(2^{iii})	0.98	3.00	3.955(5)	165.7

Symmetry operations: Bromide complex: i, 2-x, 1-y, 1-z; ii, 1-x, 1-y, 1-z; Iodide complex: i, 1-x, 1-y, 1-z; ii, x+0.5, 1.5-y, z-0.5; iii, 0.5-x, y+0.5, 1.5-z (same chain).

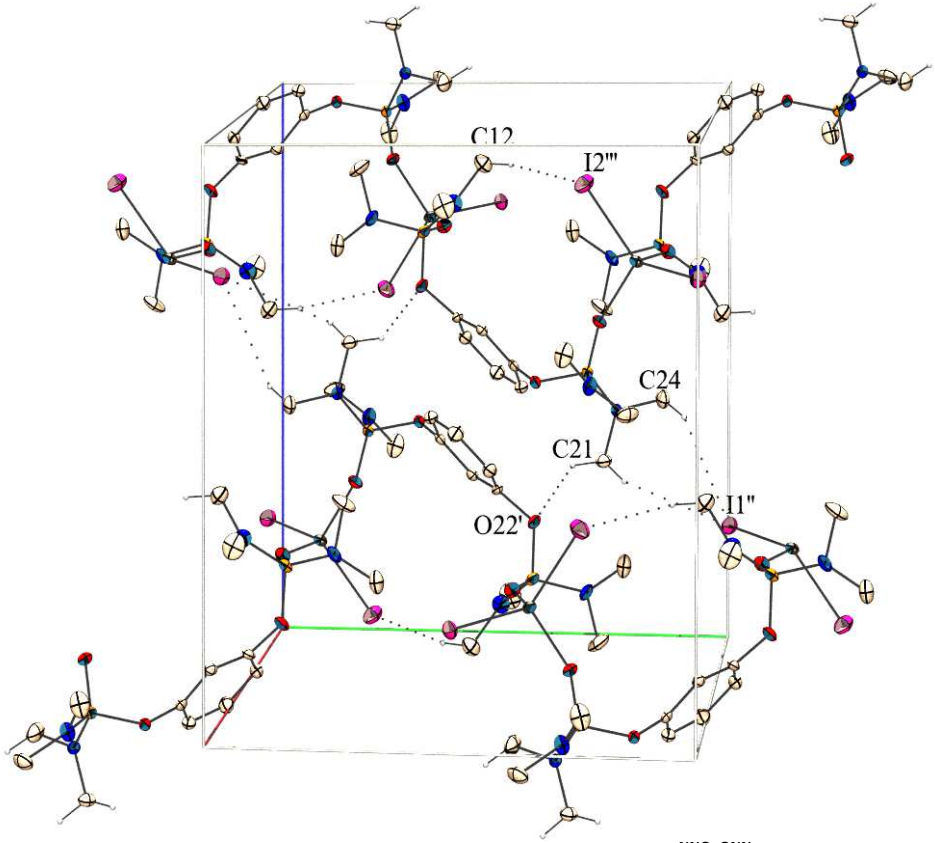

Fig. S18 The hydrogen bond network for the polymeric **$[MnI_2(\mu\text{-}OP^{NNO\sim ONN}PO)]_n$** compound.

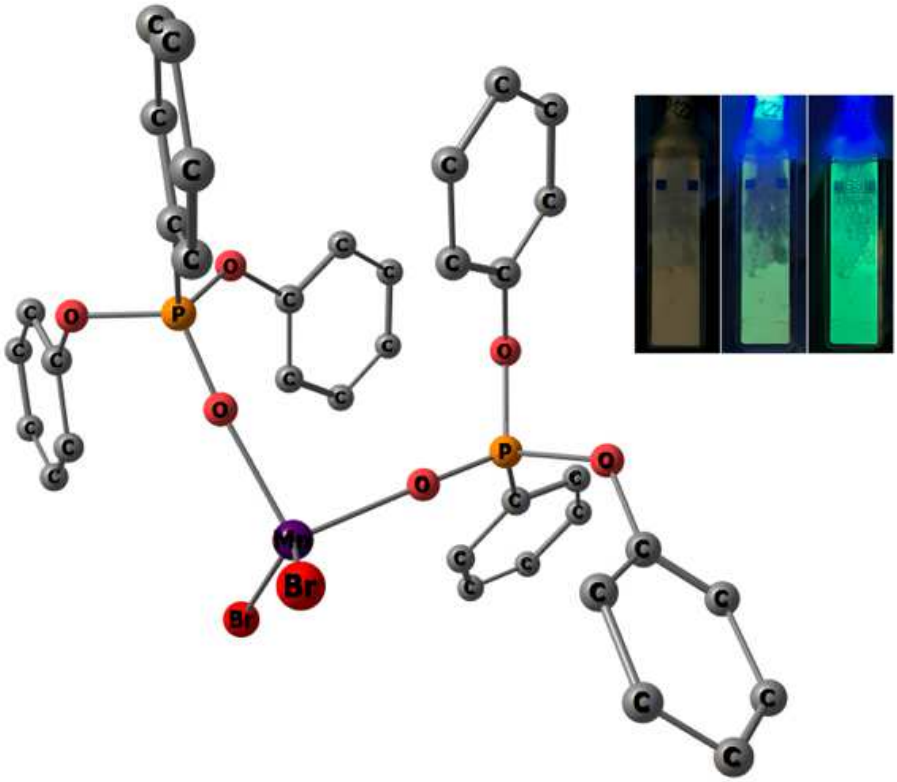

Fig. S19 DFT-optimized structure of **[$MnBr_2${OP^{COO}}$_2$]**. Hydrogen atoms are omitted for clarity. Selected computed bond lengths (Å): Mn-Br, 2.461, 2.468; Mn-O, 2.083, 2.089. Pictures of the compound under ambient (left), UV-C (central) and UV-A (right) light.

Table S7 Cartesian coordinates (Å) of the DFT-optimized structure of **[$MnBr_2${OP^{COO}}$_2$]**.

O	1.63846400	0.07837900	-0.90921900	O	-3.40464200	1.21752900	0.79587300	C	4.36555000	-1.62977400	-0.55210500
O	-1.38621300	-0.01258600	-0.27095600	O	-1.57755600	0.51006000	2.29204100	C	4.74959200	-4.37039000	-0.46209100
P	2.83964000	0.45595600	-0.10127300	O	4.20318400	-0.24216900	-0.58105100	C	5.35101500	-2.14913700	0.28113800
P	-2.28315300	0.06926700	0.92499300	O	2.72689200	0.04578100	1.44921100	C	3.57015900	-2.45084500	-1.34547100
C	-3.07951500	-1.47211100	1.32206200	C	-4.21281900	1.34170400	-0.33609700	C	3.76457000	-3.83000700	-1.28707900
C	-4.31581500	-3.88944200	1.90339400	C	-5.86367300	1.61114700	-2.54124600	C	5.54335800	-3.52842200	0.31767000
C	-3.93301500	-1.56583700	2.42973100	C	-5.57044600	1.06857400	-0.20310200	H	5.95327800	-1.46888500	0.88743900
C	-2.84654800	-2.58054300	0.50232100	C	-3.66186600	1.74986700	-1.54588300	H	2.79098100	-2.03006000	-1.98510700
C	-3.47075000	-3.79149500	0.80037600	C	-4.49893100	1.87512500	-2.65279000	H	3.12567900	-4.47634300	-1.89479500
C	-4.54838900	-2.77847900	2.71875200	C	-6.39738000	1.21162300	-1.31586600	H	6.31629500	-3.94762600	0.96741200
H	-4.10835200	-0.69271500	3.06513600	H	-5.96278400	0.75037900	0.76592400	H	4.89899700	-5.45250300	-0.42322800
H	-2.16949400	-2.50812100	-0.35641600	H	-2.59167400	1.95222400	-1.63707900	C	1.78248400	-0.75131900	2.08687900
H	-3.28928900	-4.65988500	0.16201600	H	-4.06223800	2.17846700	-3.60816900	C	-0.02421000	-2.29436900	3.52344500
H	-5.21398800	-2.86060200	3.58195100	H	-7.46671400	1.00372300	-1.22299700	C	1.51528300	-0.43402700	3.41588400
H	-4.80293300	-4.84140200	2.13270000	H	-6.51475400	1.71392100	-3.41325900	C	1.16231600	-1.82973600	1.45931000
C	3.20246900	2.19660300	-0.13839400	C	-0.90166800	1.69743000	2.53448300	C	0.25500100	-2.59516600	2.19193800
C	3.68880200	4.92814000	-0.23440200	C	0.48157700	4.01046500	3.19881400	C	0.61128900	-1.21286900	4.13298400
C	4.07446800	2.77723800	0.79060300	C	-0.13837300	2.33582600	1.55924700	H	2.01509600	0.42700000	3.86613700
C	2.56777900	2.97587300	-1.11234700	C	-0.98525000	2.19682400	3.83109200	H	1.36605300	-2.08293000	0.41623900
C	2.81925700	4.34709800	-1.15566600	C	-0.28769200	3.35528900	4.16087600	H	-0.23414900	-3.44075100	1.70044300
C	4.31494800	4.14587000	0.73939300	C	0.54974900	3.49983700	1.90428100	H	0.40030500	-0.96647900	5.17733200
H	4.55281700	2.16066100	1.55660700	H	-0.07390500	1.92729200	0.54730000	H	-0.73821900	-2.90274200	4.08486200
H	1.86721700	2.52220100	-1.82425700	H	-1.59264800	1.66212100	4.56477100	Mn	-0.13891100	-0.32605600	-1.91654100
H	2.32536000	4.95957700	-1.91415800	H	-0.35036700	3.75124800	5.17817900	Br	-0.39308500	1.63142100	-3.38674700
H	4.99298100	4.60713900	1.46204500	H	1.15013800	4.00795000	1.14412900	Br	-0.11453500	-2.76700000	-2.28035200
H	3.88115800	6.00409200	-0.27215200	H	1.02634400	4.92201500	3.45717600				

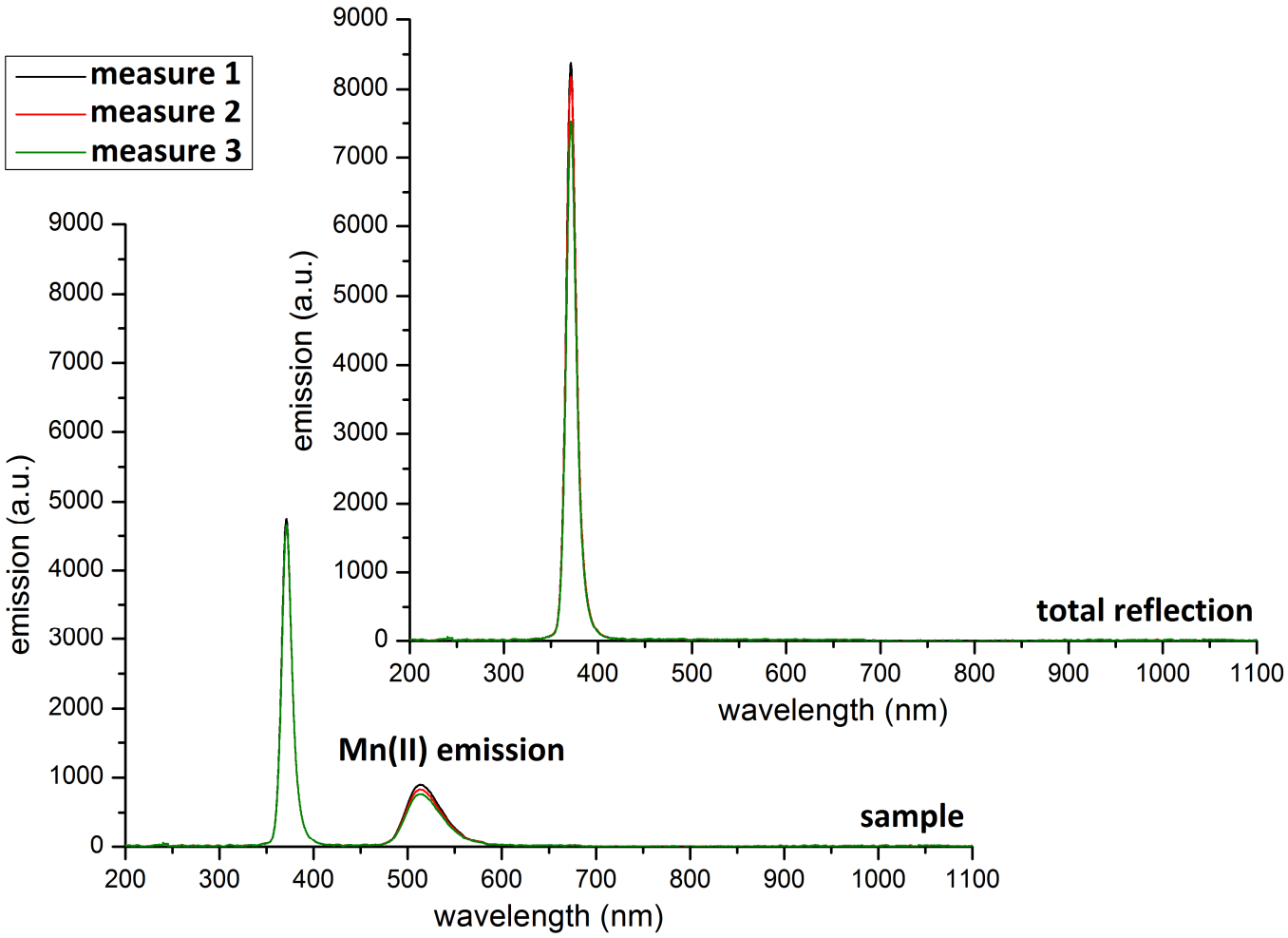

Fig. S20 Emission spectra used for the determination of $[MnI_2(OP_{NOO})_2]$ photoluminescence quantum yield.

References

1. L. J. Farrugia, *J. Appl. Crystallogr.*, 1997, **30**, 565, DOI: 10.1107/S0021889897003117; *POV-Ray v3.7 for Windows, Persistence of Vision Raytracer*, Persistence of Vision Pty. Ltd., 2016, http://www.povray.org/documentation.]

2. L. Yang, D. R. Powell and R. P. Houser, *Dalton Trans.* (2007), 955–964. DOI: 10.1039/B617136B.

3. M. Bortoluzzi and J. Castro, *J. Coord. Chem.*, 2019, **72**, 309–327, DOI: 10.1080/00958972.2018.1560430.